http://dx.doi.org/10.5012/bkcs.2013.34.12.3659

Mass Spectrometric Analysis of Eight Common Chemical Explosives Using Ion Trap Mass Spectrometer

Sehwan Park, Jihyeon Lee, Soo Gyeong Cho,† Eun Mee Goh,† Sungman Lee,‡ Sung-Suk Koh,‡ and Jeongkwon Kim*

*Department of Chemistry, Chungnam National University, Daejeon 305-764, Korea. *E-mail: jkkim48105@cnu.ac.kr*
†Agency for Defense Development, Daejeon 305-600, Korea
‡Sensor Tech Inc., Kyunggi-Do 462-713, Korea
Received August 27, 2013, Accepted September 15, 2013

Eight representative explosives (ammonium perchlorate (AP), ammonium nitrate (AN), trinitrotoluene (TNT), 2,4-dinitrotoluene (DNT), cyclonite (RDX), cyclotetramethylenetetranitramine (HMX), pentaerythritol tetranitrate (PETN), and hexanitrostilbene (HNS)) were comprehensively analyzed with an ion trap mass spectrometer in negative ion mode using direct infusion electrospray ionization. MS/MS experiments were performed to generate fragment ions from the major parent ion of each explosive. Explosives in salt forms such as AP or AN provided cluster parent ions with their own anions. Explosives with an aromatic ring were observed as either $[M–H]^-$ for TNT and DNT or $[M]^{\bullet-}$ for HNS, while explosives without an aromatic ring such as RDX, HMX, and PETN were detected as an adduct ion with a formate anion, *i.e.*, $[M+HCOO]^-$. These findings provide a guideline for the rapid and accurate detection of explosives once portable MS instruments become more readily available.

Key Words : Explosives, Electrospray ionization, Ion trap

Introduction

Rapid detection of explosives is very important due to their recent increased use for hostile purposes. Ion mobility spectrometry (IMS)[1,2] is commonly used for the detection of explosives because these devices are portable and easy to operate. In IMS, the mobility of a gaseous ion at atmospheric pressure in a weak electric field is used to characterize the ion. The limitation of IMS is its inherently limited accuracy. Mass spectrometry (MS) is used for accurate detection, but portable MS instruments have only recently appeared on the market. In this study, eight different explosives (ammonium perchlorate (AP), ammonium nitrate (AN), trinitrotoluene (TNT), 2,4-dinitrotoluene (DNT), cyclonite (RDX), cyclotetramethylenetetranitramine (HMX), pentaerythritol tetranitrate (PETN), and hexanitrostilbene (HNS)) were analyzed with an ion trap mass spectrometer using direct infusion electrospray ionization (ESI). Absolute confirmation of the explosives was obtained. This analytical approach provides a solid guideline for the rapid confirmation of explosives once portable mass spectrometers become more available.

Experimental Section

Materials. Eight different explosives (AP, AN, TNT, DNT, RDX, HMX, PETN, and HNS) were obtained from the Agency for Defense Development, South Korea. The structures of the eight explosives are provided in Figure 1. All other chemicals were purchased from Sigma-Aldrich (St. Louis, MO, USA).

Sample Preparation and Mass Spectrometry. Each explosive was dissolved to make a 10.0 μg/mL solution; acetonitrile was used as the solvent for AP, TNT, DNT,

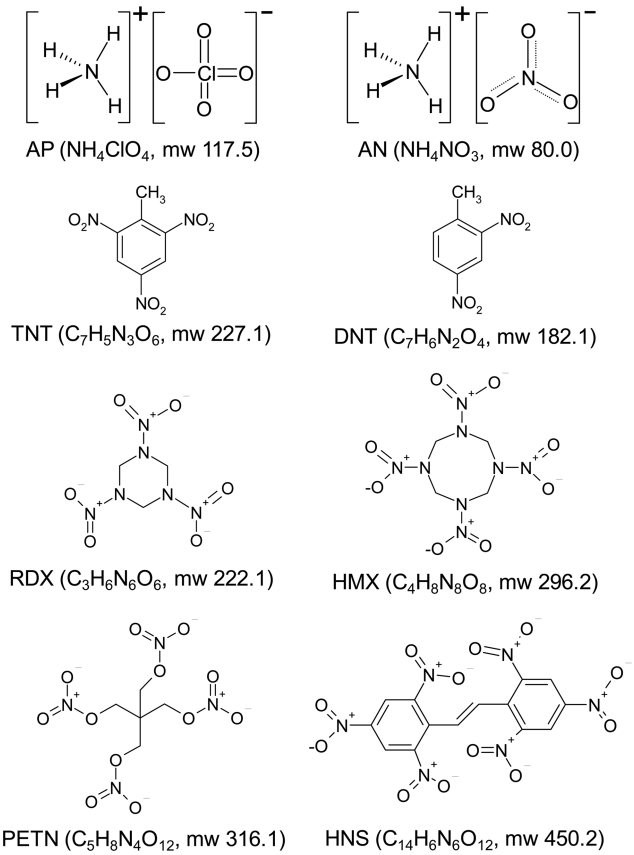

Figure 1. Structures of eight explosives investigated in the current study.

RDX, HMX, and PETN, while methanol was used for AN and HNS. The sample solution was directly infused at a flow rate of 3 μL/min into an ion trap mass spectrometer (LCQ Deca XP Plus; Thermo Finnigan, Waltham, MA, USA) with an electrospray voltage of –5 kV, a capillary temperature of 135 °C or 275 °C, a capillary voltage of –15 kV, nebulizer pressure of 100 psi, and nitrogen flow rate of 10 L/min. For the MS/MS analysis, collision-induced dissociation with a normalized collision energy of 50% was used. All acquisitions were performed in negative ion mode, scanning from *m/z* 50 to *m/z* 2000 except AN which was scanned from *m/z* 50 to *m/z* 1500.

Results and Discussion

AP. The mass spectrum of AP using ESI with *m/z* 50-2000 is shown in Figure 2(a). The pattern of the cluster ions of AP is very similar to that previously reported in which a series of cluster ions with one perchlorate anion attached was observed.[3] However, in the current analysis, we also observed cluster ions with two perchlorate anions as $(NH_4ClO_4)_m(ClO_4^-)_2$, where $m \geq 15$. These cluster ions existed in the doubly charged form. The doubly charged cluster ions with even-numbered m were observed at the same *m/z* value as the singly charged cluster ions with a half of the m value, *e.g.*, $(NH_4ClO_4)_{16}(ClO_4^-)_2$ and $(NH_4ClO_4)_8(ClO_4^-)_1$. With the current ion trap analyzer, distinguishing the two peaks is impossible. Experiments using a mass analyzer with increased resolution such as time-of-flight, Orbitrap, or Fourier transform ion cyclotron resonance can resolve the two peaks.

When the scan range was narrowed to *m/z* 50-1500, a prominent peak at *m/z* 99.2 from the ClO_4^- ion was observed (Fig. 2(b)). The ion trap scanning from *m/z* 50 to *m/z* 2000 was assumed to not have effectively stored the ion with *m/z* 99.2 because of the low mass cutoff in the ion trap.[4] The relative abundance of the two peaks generated by the presence of one chlorine was 1.00:0.37 (for the peaks of $^{35}ClO_4^-$:$^{37}ClO_4^-$), which closely corresponds to the natural isotopic abundance of ^{35}Cl:^{37}Cl (1.00:0.32). The fragmentation of the peak at *m/z* 99.2 provided no peaks, while the fragmentation of the peak at *m/z* 215.8 from $(NH_4ClO_4)(ClO_4^-)$ gave two dominant fragment peaks at *m/z* 198.8 for $(HClO_4)(ClO_4^-)$ and at *m/z* 99.5 for ClO_4^- (Fig. 2(c)).

AN. Figure 3(a) shows the mass spectrum of AN, which was observed with the capillary temperature of 135 °C. When the temperature was 275 °C, which is the typical setting for an ESI-MS experiment, no peak from AN was detected. The observation of cluster ions of AN at a lower temperature was previously reported[5] when a capillary temperature of 100 °C was used to detect cluster ions. AN is known to decompose into nitrous oxide and water at about 210 °C.[3] The fragmentation of the peaks at *m/z* 186.9 from $(HNO_3)_2(NO_3^-)$ and at *m/z* 125.0 from $(HNO_3)(NO_3^-)$ generated product ion peaks at *m/z* 125.1 from $(HNO_3)(NO_3^-)$ (Fig. 3(b)) and at *m/z* 62.2 for NO_3^- (Fig. 3(c)).

TNT. The mass spectrum of TNT is shown in Figure 4.

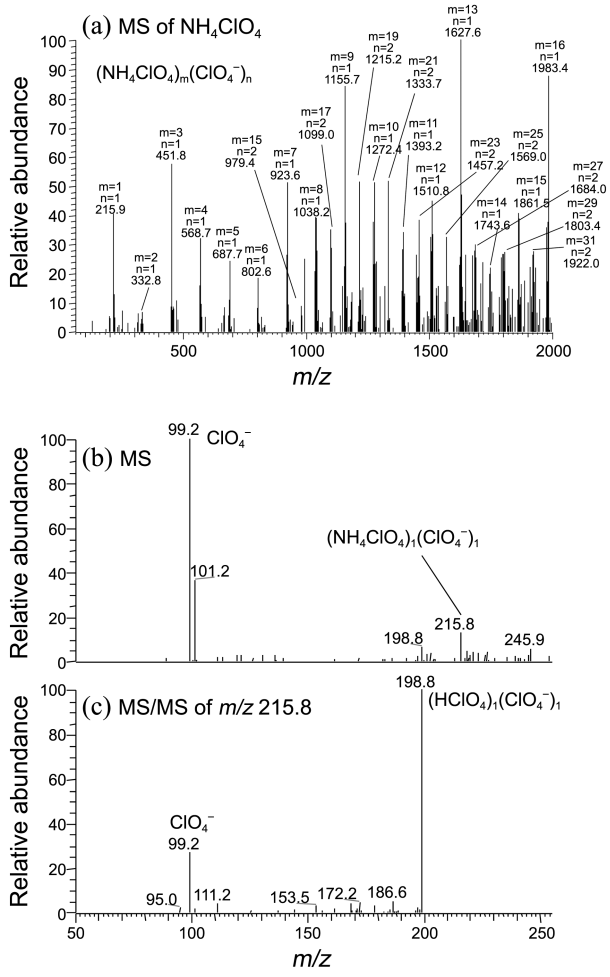

Figure 2. Negative-ion ESI mass spectra of AP. (a) Mass spectrum from *m/z* 50 to *m/z* 2000; (b) mass spectrum from *m/z* 50 to *m/z* 250, where the original data were acquired from *m/z* 50 to *m/z* 1500, and (c) MS/MS spectrum of *m/z* 215.8.

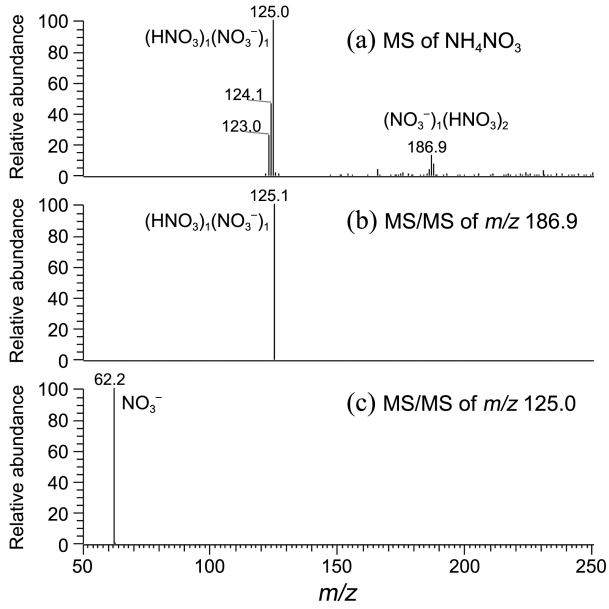

Figure 3. Negative-ion ESI mass spectra of AN. (a) Mass spectrum, (b) MS/MS spectrum of *m/z* 186.9, and (c) MS/MS spectrum of *m/z* 125.0.

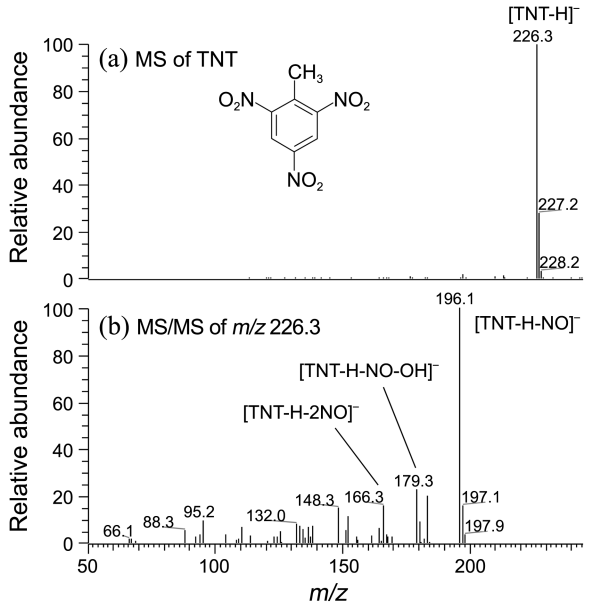

Figure 4. Negative-ion ESI mass spectra of TNT. (a) Mass spectrum and (b) MS/MS spectrum of *m/z* 226.3.

TNT was observed in the deprotonated form, providing $[TNT–H]^-$ at *m/z* 226.3. Fragmentation of $[TNT–H]^-$ provided a dominant fragment peak at *m/z* 196.1, which was assigned to $[TNT–H–NO]^-$, and two minor peaks at *m/z* 179.3 and *m/z* 166.3 corresponding to $[TNT–H–NO–OH]^-$ and $[TNT–H–2NO]^-$, respectively.

Observation of $[TNT–H]^-$ with ESI in the negative ion mode was previously reported.[6,7] The fragmentation of $[TNT–H]^-$ reportedly provided fragment ions at *m/z* 198 $[TNT–H–CO]^-$ and *m/z* 196 $[TNT–H–NO]^-$.[6] Atmospheric pressure chemical ionization (APCI) analysis of TNT in the negative ion mode gave the $[TNT]^-$ ion.[6,8]

DNT. The mass spectrum of DNT provided the deprotonated ion peak at *m/z* 181.3 $[DNT–H]^-$ as shown in Figure 5(a). The MS/MS spectrum of the peak at *m/z* 181.3 $[DNT–H]^-$ is shown in Figure 5(b), where two dominant fragment peaks are present at *m/z* 152.3 for $[DNT–NO]^-$ and *m/z* 116.3 for $[DNT–2H_2O–NO]^-$.

The observation of $[DNT–H]^-$ with ESI in negative ion mode was previously described.[7] However, no MS/MS fragmentation of the parent ion generated using ESI has been reported. We only found literature regarding MS/MS analysis of DNT using APCI and low-temperature plasma (LTP) ambient ionization. APCI analysis of DNT generated $[DNT]^{\bullet-}$ at *m/z* 182 and the MS/MS experiment of $[DNT]^{\bullet-}$ provided $[DNT–HNO_2]^-$ at *m/z* 135, $[DNT–NO–CH_3]^-$ at *m/z* 137, $[DNT–NO]^-$ at *m/z* 152, $[DNT–H_2O]^-$ at *m/z* 164, and $[DNT–OH]^-$ at *m/z* 165.[8] LTP ambient ionization of DNT produced the $[DNT–H]^-$ ion, whereby the MS/MS spectrum for *m/z* 181 from $[DNT–H]^-$ yielded a product ion at *m/z* 116.[9]

RDX and HMX. The mass spectra of RDX and HMX are shown in Figures 6 and 7, respectively. Although no formate was added to the samples, the dominant peaks for RDX and HMX were observed as the formate adduct ions $[M+HCOO]^-$ at *m/z* 267.0 and *m/z* 341.1, respectively. The formate adduct ions of RDX and HMX were previously observed in the analysis using direct-infusion ESI–Fourier transform ion cyclotron resonance MS,[10] whereby the generation of formate adduct ions was attributed to the decomposition of RDX or HMX. The peak at *m/z* 267 in the analysis of RDX and that at *m/z* 341 in the analysis of HMX were incorrectly assigned as $[RDX+NO_2–H]^-$ and $[HMX+NO_2–H]^-$, respectively, in a previous study.[11] The mass difference between $[HCOO]^-$ (44.998 amu) and $[NO_2–H]^-$ (44.986 amu) is only 0.012 amu. The advent of high-accuracy FT-ICR MS has now correctly identified the peaks

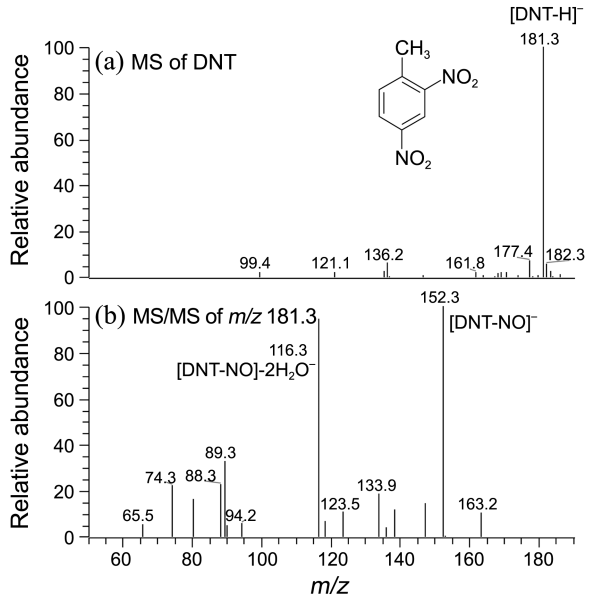

Figure 5. Negative-ion ESI mass spectra of DNT. (a) Mass spectrum and (b) MS/MS spectrum of *m/z* 181.3.

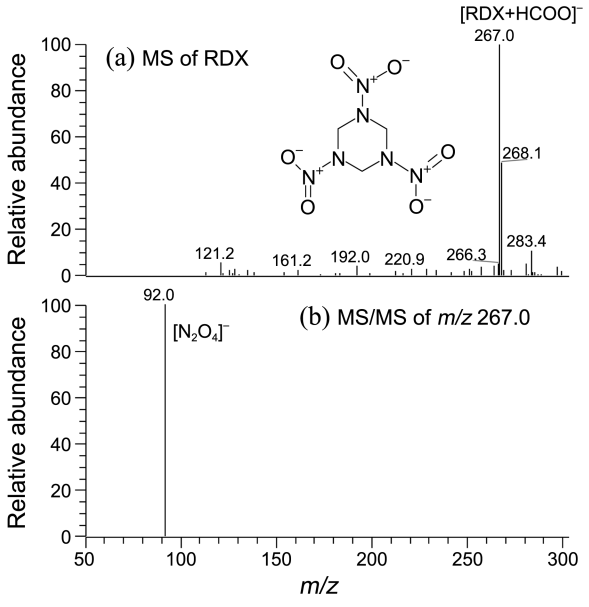

Figure 6. Negative-ion ESI mass spectra of RDX. (a) Mass spectrum and (b) MS/MS spectrum of *m/z* 267.0. RDX was observed as a formate adduct ion.

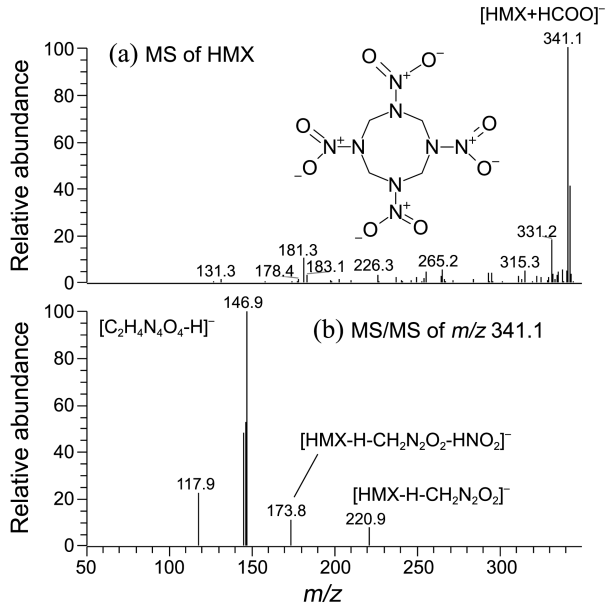

Figure 7. Negative-ion ESI mass spectra of HMX. (a) Mass spectrum and (b) MS/MS spectrum of *m/z* 341.1. HMX was observed as a formate adduct ion.

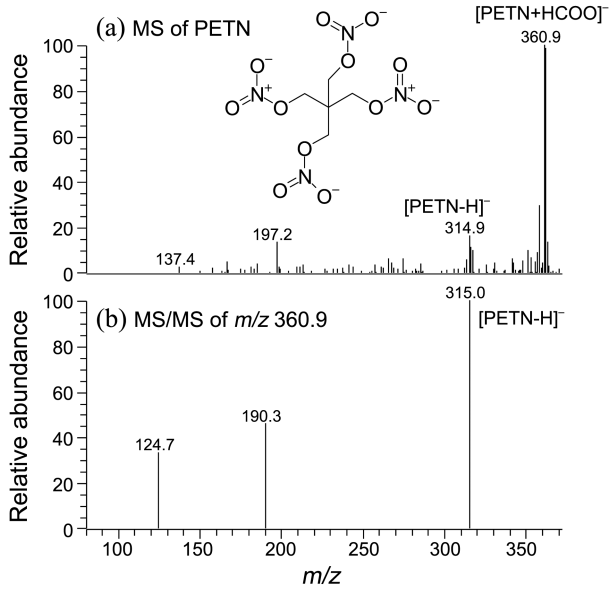

Figure 8. Negative-ion ESI mass spectra of PETN. (a) Mass spectrum and (b) MS/MS spectrum of *m/z* 360.9. PETN was observed as a formate adduct ion.

as $[M+HCOO]^-$ ions.[10] The presence of formate could also be due to a trace amount of formic acid left from previous experiments. Even though the system was thoroughly cleaned with acetonitrile, methanol, and water for the current investigation, it is possible that a trace level of formic acid still exists in the system as an impurity. Further investigation is needed to confirm the origin of formate.

RDX and HMX were often detected as $[M+Cl]^-$ ions in ESI analyses, whereby the chloride was assumed to be an impurity from leaching from the glass vials or from a sample.[7,10] To improve the signals of the $[M+Cl]^-$ ions, chloride ions were often intentionally added.[7] Recently, the addition of HCl to the spray solvent in the DESI analysis of RDX and HMX provided $[M+^{35}Cl]^-$ and $[M+^{37}Cl]^-$ ions.[12]

In the analysis of HMX using ESI-MS under negative ion mode, HMX was always detected as an adduct ion with an anion, whereby various anions such as formate, acetate, propionate, nitrate, nitrite, or chloride were used as an additive to form the adduct anion.[13]

Fragmentation of $[RDX+HCOO]^-$ provided a peak at *m/z* 92.0 $[N_2O_4]^-$ (Fig. 6(b)). Fragmentation of $[HMX+HCOO]^-$ provided peaks at *m/z* 146.9 $[C_2H_3N_4O_4]^-$, *m/z* 173.8 $[HMX–H–CH_2N_2O_2–HNO_2]^-$, and *m/z* 146.9 $[HMX–H–CH_2N_2O_2]^-$ (Fig. 7(b)), whereby the fragmentation pattern of $[HMX+HCOO]^-$ is very similar to that of $[HMX+CH_3COO]^-$ reported previously.[14]

PETN. MS analysis of PETN provided a main peak at *m/z* 360.9 $[PETN+HCOO]^-$ as an adduct peak with a formate ion; a small peak at *m/z* 314.9 $[PETN–H]^-$ was also observed as shown in Figure 8(a). MS/MS analysis of the peak at *m/z* 360.9 provided a fragment ion peak at *m/z* 315.0 $[PETN–H]^-$ as shown in Figure 8(b).

Few studies have been reported concerning the MS analysis of PETN, probably because of its difficulty to ionize. In DESI analysis, PETN was observed as $[M–H]^-$ or $[M+Cl]^-$, when the chloride ion was assumed to be intentionally added to the spray solvent.[12] In LTP analysis, PETN was observed as $[M+NO_2]^-$ or $[M+NO_3]^-$, whereby NO_2^- or NO_3^- was generated from the ionization of air.[9] In ESI analysis, PETN was observed as $[M–H]^-$, $[M+HCOO]^-$, and $[M+CH_3COO]^-$.[11]

HNS. MS analysis of HNS provided two dominant peaks at *m/z* 402.2 $[M–NO–H_2O]^-$ and at *m/z* 420.1 $[M–NO]^-$, with

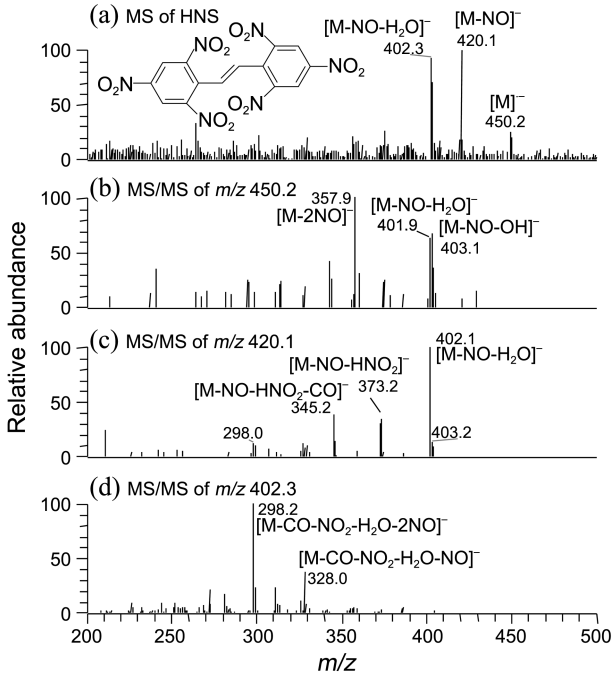

Figure 9. Negative-ion ESI mass spectra of HNS. (a) Mass spectrum, (b) MS/MS spectrum of *m/z* 450.2, (c) MS/MS spectrum of *m/z* 420.1, and (d) MS/MS spectrum of *m/z* 402.3.

Table 1. Summary of the MS and MS/MS data for eight explosives

Explosive	Parent ions	Daughter ions
AP	$(NH_4ClO_4)_m(ClO_4^-)_n$, where m = 0 to 31 and n = 1, 2	
	215.8 $[(NH_4ClO_4)(ClO_4)]^-$	198.8 $[(HClO_4)_1(ClO_4)]^-$ (12.9%) 99.2 $[ClO_4]^-$ (100.0%)
AN	186.9 $[(HNO_3)_2(NO_3)]^-$ (12.9%)	125.1 $[(HNO_3)(NO_3)]^-$ (100.0%)
	125.0 $[(HNO_3)(NO_3)]^-$ (100.0%)	62.2 $[NO_3]^-$ (100.0%)
TNT	226.3 $[M-H]^-$	196.1 $[M-H-NO]^-$ (100.0%) 179.3 $[M-H-NO-OH]^-$ (22.7%) 166.3 $[M-H-2NO]^-$ (16.0%)
DNT	181.3 $[M-H]^-$	152.3 $[M-NO]^-$ (100.0%) 116.3 $[M-NO-2H_2O]^-$ (94.7%)
RDX	267.0 $[M+HCOO]^-$	92.0 $[N_2O_4]^-$ (100.0%)
HMX	341.1 $[M+HCOO]^-$	220.9 $[M-H-CH_2N_2O_2]^-$ (7.4%) 173.8 $[M-H-CH_2N_2O_2-HNO_2]^-$ (10.8%) 146.9 $[C_2H_4N_4O_4-H]^-$ (100.0%)
PETN	360.9 $[M+HCOO]^-$	315.0 $[M-H]^-$ (100.0%)
HNS	450.2 $[M]^{\bullet-}$ (24.5%)	403.1 $[M-NO-OH]^-$ (67.0%) 401.9 $[M-NO-H_2O]^-$ (63.0%) 357.9 $[M-2NO]^-$ (100.0%)
	420.1 $[M-NO]^-$ (100.0%)	402.3 $[M-NO-H_2O]^-$ (100.0%) 373.2 $[M-NO-HNO_2]^-$ (34.3%) 345.2 $[M-NO-HNO_2-CO]^-$ (37.7%)
	402.3 $[M-NO-H_2O]^-$ (92.5%)	328.0 $[M-CO-NO_2-H_2O-NO]^-$ (37.5%) 298.2 $[M-CO-NO_2-H_2O-2NO]^-$ (100.0%)

a small peak at *m/z* 450.2 $[M]^{\bullet-}$ as shown in Figure 9(a). The $[M]^{\bullet-}$ and $[M–NO–H_2O]^-$ ions have already been reported.[6]

MS/MS analysis for the peak at *m/z* 450.2 provided fragment ion peaks at *m/z* 403.1 $[M–NO–OH]^-$, *m/z* 401.9 $[M–NO–H_2O]^-$, and *m/z* 357.9 $[M–2NO]^-$. MS/MS analysis for the peak at *m/z* 420.1 provided fragment ion peaks at *m/z* 402.1 $[M–NO–H_2O]^-$, *m/z* 373.2 $[M–NO–HNO_2]^-$, and at *m/z* 345.2 $[M–NO–HNO_2–CO]^-$. MS/MS analysis for the peak at *m/z* 402.3 provided two main fragment ion peaks at *m/z* 328.0 $[M–CO–NO_2–H_2O–NO]^-$ and at *m/z* 298.2 $[M–CO–NO_2–H_2O–2NO]^-$. The detailed MS/MS spectra are provided in Figure 9(b-d).

In summary, Table 1 provides details of the MS and MS/MS analysis of the eight explosives. Explosives such as AP and AN in the form of salts were detected in the MS analysis as cluster ions with their own anions. The MS/MS analysis of the parent ions in the MS analysis of AP and AN provided fragment ion peaks generated from the neutral loss of NH_3 or NH_4ClO_4 for AP or HNO_3 for AN. Explosives with an aromatic ring were detected as either a deprotonated anion $[M–H]^-$ for TNT and DNT or an electron-attached radical anion $[M]^{\bullet-}$ for HNS, whereby the aromatic ring is believed to stabilize the $[M–H]^-$ or $[M]^{\bullet-}$ ions. The MS/MS analysis of the parent ions from the MS analysis of TNT, DNT, and HNS showed fragment ions with a loss of NO and its subsequent losses. Explosives without an aromatic ring such as RDX, HMX, and PETN were detected as adducts with a formate ion, *i.e.*, $[M+HCOO]^-$.

Conclusions

Extensive MS and MS/MS analyses of eight common explosives were performed using an ion trap mass spectrometer with electrospray ionization in negative ion mode. The parent ions of the explosives were observed as cluster ions for AP and AN, as $[M–H]^-$ for TNT and DNT, as $[M]^{\bullet-}$ for HNS, and as $[M+HCOO]^-$ for RDX, HMX, and PETN. These findings provide a guideline for the rapid and accurate detection of explosives using portable MS instruments.

Acknowledgments. This project was financially supported by the Agency for Defense Development.

References

1. Makinen, M. A.; Anttalainen, O. A.; Sillanpaa, M. E. T. *Anal. Chem.* **2010**, *82*, 9594.
2. Armenta, S.; Alcala, M.; Blanco, M. *Anal. Chim. Acta* **2011**, *703*, 114.
3. Zhao, X.; Yinon, J. *Rapid Commun. Mass Spectrom.* **2002**, *16*, 1137.
4. Kim, J.; Kim, J.; Hong, J.; Lee, S.; Park, S.; Lee, J.-H.; Kim, J. *Carbohyd. Res.* **2013**, *372*, 23.
5. Zhao, X.; Yinon, J. *Rapid Commun. Mass Spectrom.* **2001**, *15*, 1514.
6. Fu, X.; Zhang, Y.; Shi, S.; Gao, F.; Wen, D.; Li, W.; Liao, Y.; Liu, H. *Rapid Commun. Mass Spectrom.* **2006**, *20*, 2906.
7. Reid Asbury, G.; Klasmeier, J.; Hill, H. H., Jr. *Talanta* **2000**, *50*, 1291.

8. Zhao, X.; Yinon, J. *J. Chromatogr. A* **2002**, *946*, 125.
9. Garcia-Reyes, J. F.; Harper, J. D.; Salazar, G. A.; Charipar, N. A.; Ouyang, Z.; Cooks, R. G. *Anal. Chem.* **2011**, *83*, 1084.
10. Wu, Z.; Hendrickson, C. L.; Rodgers, R. P.; Marshall, A. G. *Anal. Chem.* **2002**, *74*, 1879.
11. Yinon, J.; McClellan, J. E.; Yost, R. A. *Rapid Commun. Mass Spectrom.* **1997**, *11*, 1961.
12. Cotte-Rodriguez, I.; Takats, Z.; Talaty, N.; Chen, H. W.; Cooks, R. G. *Anal. Chem.* **2005**, *77*, 6755.
13. Pan, X.; Tian, K.; Jones, L. E.; Cobb, G. P. *Talanta* **2006**, *70*, 455.
14. Pan, X.; Zhang, B.; Tian, K.; Jones, L. E.; Liu, J.; Anderson, T. A.; Wang, J.-S.; Cobb, G. P. *Rapid Commun. Mass Spectrom.* **2006**, *20*, 2222.